

## Dual Array Microseismic Hydraulic Fracture Imaging

Shawn Maxwell\*

Pinnacle Technologies, Calgary, AB  
shawn.maxwell@pinntech.com

U. Zimmer

Pinnacle Technologies, Calgary, AB, Canada

and

J. Wolfe

BP North America Gas, Calgary, AB, Canada

### Summary

A hydraulic fracture stimulation was monitored with borehole geophone arrays deployed in two observation wells. The resulting case study allowed a comparison of accuracies from single observation wells with that from two observation wells. A comparison was also made of the accuracy of the different well configurations. The dual well observations provides an opportunity for enhanced velocity model validation in addition to enhanced source imaging techniques to provide additional information about the fracture geometry.

### Introduction

The effectiveness of a hydraulic fracture stimulation is critical for optimal economic tight gas production. Deformation associated with fracturing results in small magnitude micro-earthquakes that can be used to image the fracture network. Fracture networks can be imaged based on the distribution of hypocentral event locations, although other seismic signal attributes can also be used to provide additional constraints on the fracture geometry.

Hydraulic fractures are generally formed through tensile fracturing resulting from injection of pressurized fluids, and tend to form orthogonal to the minimum principle stress direction. However, in naturally fractured reservoirs there may also be significant fracture complexity as the injection interacts with the pre-existing fracture network. The orientation of a hydraulic fracture can be mapped through alignment of microseismic event locations. Additionally, microseismic signal attributes, such as the radiation pattern of compressional and shear waves can be used to constrain the fracture plane orientation using focal mechanism techniques (see Maxwell et al., 2007). Most microseismic hydraulic fracture imaging uses geophones in a single wellbore, however if more observation wells are available improved seismic detection and imaging can be obtained. Furthermore, improved sampling of the seismic radiation pattern can be achieved for improved focal mechanism calculations.

Here we present a case study where microseismic imaging was used to image the geometry of a hydraulic fracture. A dual monitoring array was used, the advantages of which are highlighted in this paper.

## Case Study

The monitoring used two arrays of 32 triaxial geophones in each of two wells. The signals from each well were acquired on a single acquisition system to provide a common sampling timebase, necessary for arrival time inversion of microseismic event locations using both wells. Unlike single well monitoring where polarization directions are required with the arrival time inversion to constrain the location, dual array monitoring is able to constrain the microseismic location based on arrival times only. Wolfe et al. 2007, describe the results of the imaging of the fracture network.

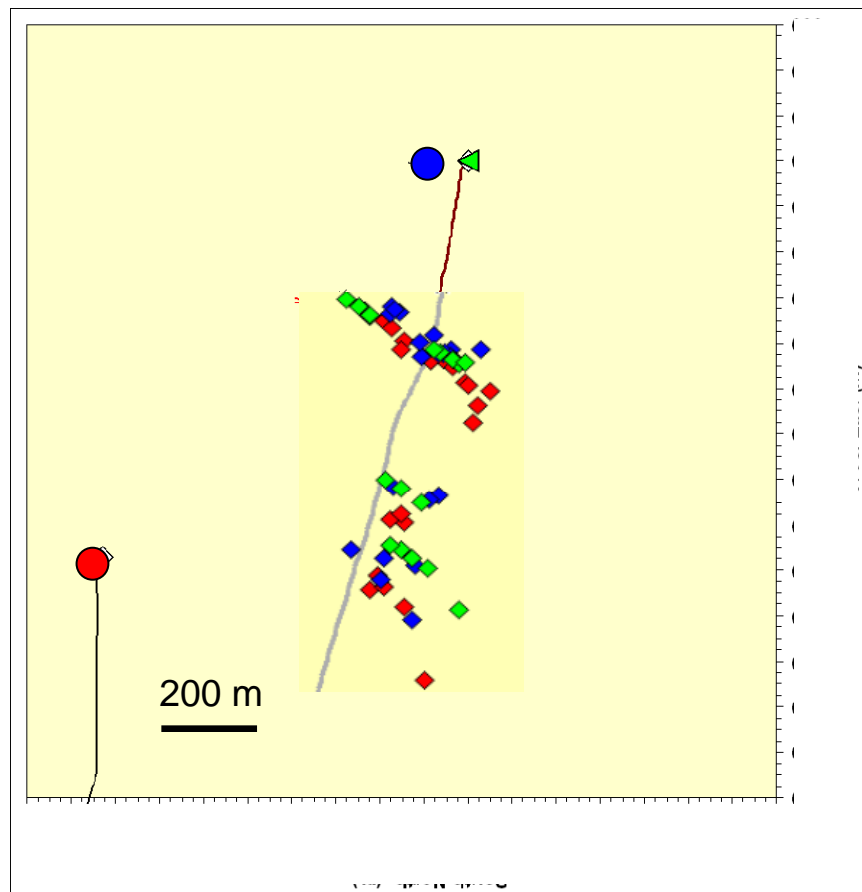


Figure 1: Map view of high quality event locations computed from both wells combined (green) and each of the single observation wells (red and blue).

Figure 1 shows a map view of a subset of the events, with very high signal-to-noise ratios across both arrays. Event locations were computed by inverting the arrival times in both wells (green symbols in Figure 1). Locations were also computed for both of the individual wells, to simulate the locations that could be obtained from single wells (red and blue symbols in Figure 1). Such a comparison allows confirmation of the individual sets of locations as well as validation of the velocity model used in the processing. If the velocity model is correct, the three sets of locations will overlap.

An important aspect of microseismic interpretation is consideration of the location uncertainties. Figure 2 shows location uncertainties for the dual array events in Figure 2. For two particular events (large symbol) contours are plotted of mismatches between observed phase arrival times and predicted times for each point in space. The hypocentral location is the point of minimal arrival time mismatch, and the contour lines define the shape of the error ellipsoid. Monte Carlo error analysis was also performed, results of which are shown by the smaller symbols. Notice that the selected event, which is offset from the frac well, has a larger location uncertainty. Furthermore, the direction of maximum uncertainty is in a direction parallel to lineations apparent from the microseismic events in Figure 1. This location uncertainty will tend artificially spread the events out in the same direction as the overall hydraulic fracture orientation.

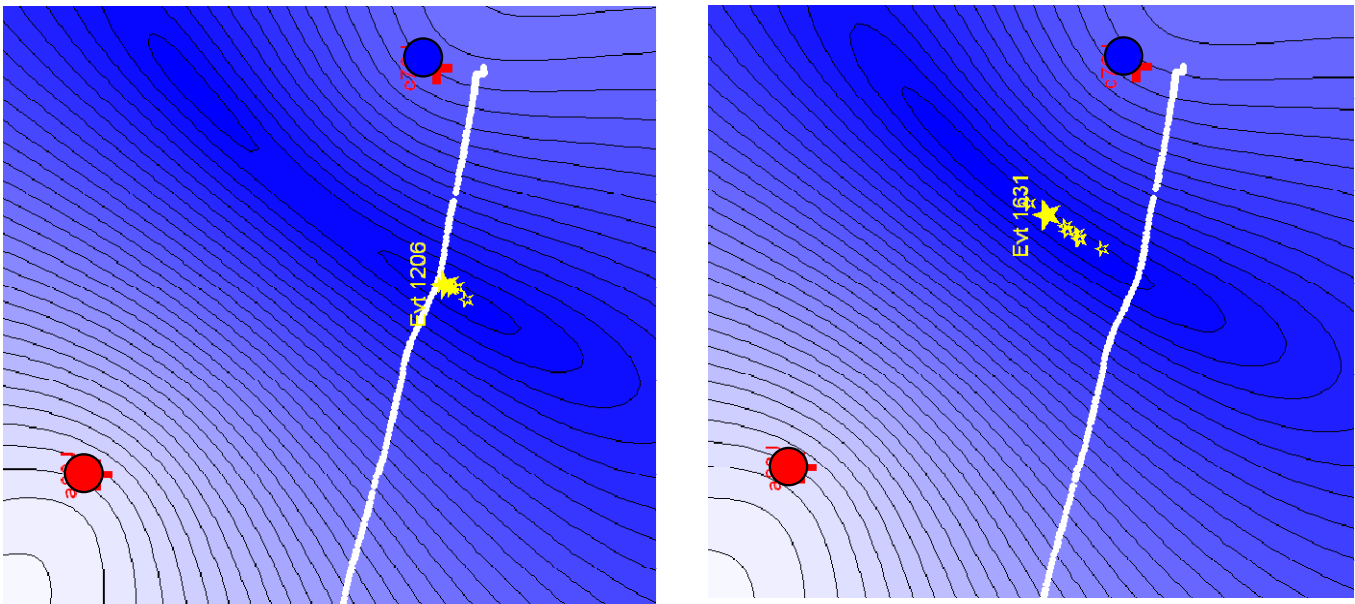


Figure 2: Arrival time mismatch contours and Monte Carlo error estimates (small symbols) for two events (large symbols).

The dual array data also enabled reliable focal mechanism determination. Relative amplitude ratios of p- to s-waves, s-wave polarizations and first breaks were used to constrain the fault plane determination. Individual events result in identification of both a primary and conjugate fracture plane. Stress inversions were performed to determine the fracture plane most consistent with a single stress field. Figure 3 shows the orientation of the constrained fracture planes (red) and conjugate planes (black). The focal mechanisms were predominantly characterized by a strike-slip failure mechanism which is consistent with regional stress field of the area. Notice that the orientation of the fracture planes is parallel to the direction of lineations of the individual events in Figure 1, confirming the fracture orientation.

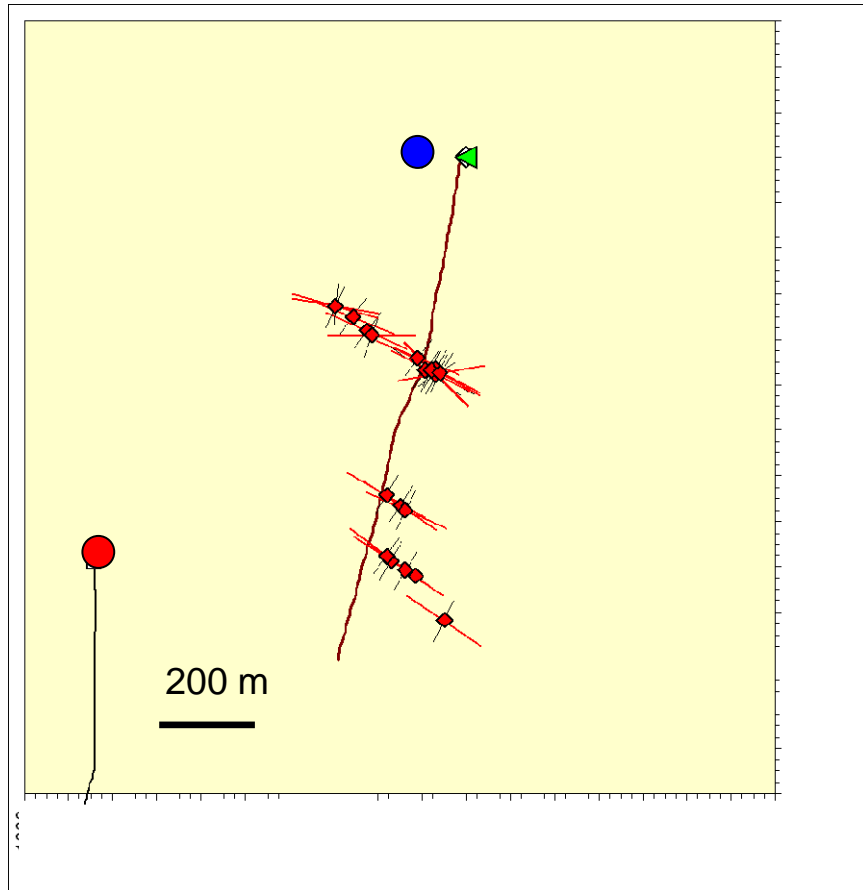


Figure 3: Strike of fractures determined from fault plane solutions.

### References

- Wolfe, J.,E. Maxwell, S.C., and Zimmer, U., 2007, Microseismic Measurement of Fracture Geometry using Synchronized Three Component Geophone Extended Arrays, CSEG abstract.
- Maxwell, S.C., Zimmer, U., Gusek, R. and Quirk, D., 2007, Evidence of a Horizontal Hydraulic Fracture at Depth Due to Stress Rotations Across a Thrust Fault, SPE 110696.